[3]Fang, T. and Wang, Z. N., "A Generalization of Caughey's Normal Mode Approach to Nonlinear Random Vibration Problems," to be published in *AIAA Journal*.

[4]Caughey, T. K., "Equivalent Linearization Techniques," *Journal of the Acoustical Society of America*, Vol. 35, No. 11, 1963, pp. 1706-1711.

Finite Element Analysis of Elastoplastic Contact Problems with Friction

Pwu Tsai* and Wen-Hwa Chen†
National Tsing Hua University
Hsinchu, Taiwan, China

Introduction

THE aim of this Note is to extend the authors' previous work[1] analyzing elastodynamic sliding contact problems with friction to deal with static small deformation elastoplastic problems. In this work, the deformed contact areas are obtained by the constraint conditions developed by a quadratic mathematic programming technique.[2] Lagrangian multipliers are introduced to evaluate the contact pressures due to friction and determine the adhesion or release of contact surface. The plastic behaviors in the contact components are accurately modeled. The influence of material properties and friction effects on the plastic zones and deformations is discussed. This is of practical importance in designing the optimum metal-forming process, especially when using a deformable die, a case which is seldom solved in literature.[3]

Finite Element Formulation

Following the procedure developed by the authors,[1] the governing equations for elastoplastic contact problems with friction can be written as

$$\frac{\partial \Pi_M}{\partial \{\Delta U_i \atop T_S\}} = 0 \tag{1}$$

$$\sum_{\ell=1}^{L} \int_{S_{C\ell}} \lambda [\mathfrak{F}(X_{Di}^{(N+1)}) - \mathfrak{F}(X_{Wi}^{(N+1)})] \, dS = 0 \tag{2}$$

$$\sum_{\ell=1}^{L} \int_{S_{C\ell}} [\mathfrak{F}(X_{Di}^{(N+1)}) - \mathfrak{F}(X_{Wi}^{(N+1)})] \, dS \geq 0 \tag{3}$$

and

$$\lambda \geq 0 \tag{4}$$

where ΔU_i are the incremental displacement components from the Nth load step to the $(N+1)$th step; T_S the Lagrangian multiplier, which can be shown to be the tangential contact pressure due to friction; λ another Lagrangian multiplier used to relax the condition of non-interpenetration on element contact surface $S_{C\ell}$; L the total number of element contact surfaces; and $\mathfrak{F}$ the contact surface function that is taken to establish the non-interpenetration conditions between components D and W. The variables $X_{Di}^{(N+1)}$, $X_{Wi}^{(N+1)}$ represent the Cartesian coordinates of the material points in contact components D and W. The functional Π_M can be expressed as

$$\begin{aligned}\Pi_M(\Delta U_i, T_S, \lambda) = &\sum_{n=1}^{N_D} \left[\int_{\Omega Dn} \left(\frac{1}{2} \Delta\sigma_{ij} \Delta\epsilon_{ij} \right) dV \right. \\ &\left. - \int_{S_{\sigma Dn}} (\Delta \bar{T}_i \Delta U_i) \, dS + \epsilon_{Dn}^{(N)} \right] \\ &+ \sum_{n=1}^{N_W} \left[\int_{\Omega Wn} \left(\frac{1}{2} \Delta\sigma_{ij} \Delta\epsilon_{ij} \right) dV \right. \\ &\left. - \int_{S_{\sigma Wn}} (\Delta \bar{T}_i \Delta U_i) \, dS + \epsilon_{Wn}^{(N)} \right] \\ &- \sum_{\ell=1}^{L} \left[\int_{S_{C\ell}} T_S (\Delta U_{DS} - \Delta U_{WS}) \, dS \right] \\ &- \sum_{\ell=1}^{L} \left[\int_{S_{C\ell}} \lambda (\mathfrak{F}(X_{Di}^{(N+1)}) - \mathfrak{F}(X_{Wi}^{(N+1)}) \, dS \right]\end{aligned}$$

where

$$\epsilon_{Dn}^{(N)} = \int_{\Omega Dn} \sigma_{ij}^{(N)} \Delta\epsilon_{ij} \, dV - \int_{S_{\sigma Dn}} \bar{T}_i^{(N)} \Delta U_i \, dS$$

$$\epsilon_{Wn}^{(N)} = \int_{\Omega Wn} \sigma_{ij}^{(N)} \Delta\epsilon_{ij} \, dV - \int_{S_{\sigma Wn}} \bar{T}_i^{(N)} \Delta U_i \, dS$$

ΔU_i, T_S, and λ are treated as independent variables in Π_M. $(N_D, \Omega_{Dn}, S_{\sigma Dn})$ and $(N_W, \Omega_{Wn}, S_{\sigma Wn})$ represent the total number of elements, element domains, and element traction surfaces of components D and W, respectively. $\Delta\sigma_{ij}$ and $\Delta\epsilon_{ij}$ are the incremental stress and strain tensors from the Nth load step to the $(N+1)$th step, and $\Delta\bar{T}_i$ are the incremental prescribed tractions from the Nth load step to the $(N+1)$th step. $\epsilon_{Dn}^{(N)}$ and $\epsilon_{Wn}^{(N)}$ are the correction terms to do the equilibrium check of components D and W at the Nth load step incurred by nonlinear plastic behaviors. $\sigma_{ij}^{(N)}$ is the stress tensor and $\bar{T}_i^{(N)}$ are the total prescribed tractions at the Nth load step. The tangential components of incremental displacements ΔU_i on contact surfaces of components D and W are denoted as ΔU_{DS} and ΔU_{WS}, respectively.

Closely following the authors' earlier work,[1] some tedious manipulations resulted in the final simultaneous algebraic equations and constraints

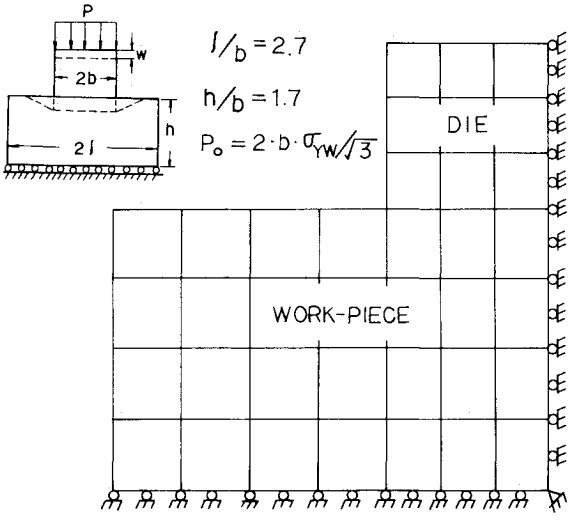

Fig. 1 ADINA's punch problem.

Received Feb. 15, 1985; revision received April 8, 1985.

*Graduate Student, Department of Power Mechanical Engineering.
†Professor and Head, Department of Power Mechanical Engineering.

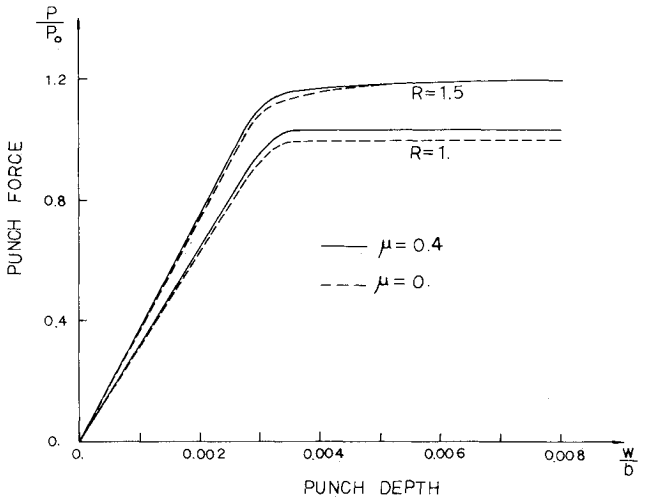

Fig. 2 Punch forces vs punch depths for different material ratios R and friction coefficients μ.

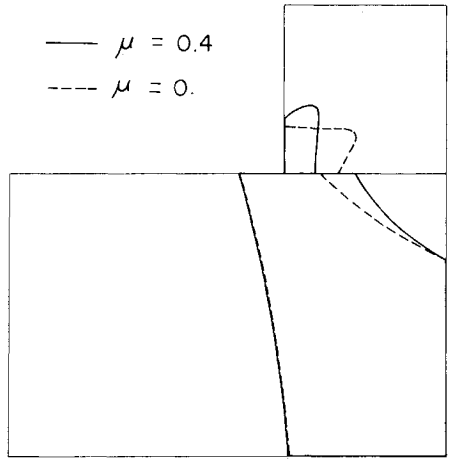

Fig. 3 Influence of friction coefficients on the spreading of plastic zones ($R=1.5$, $W/b=0.008$).

equations and constraints

$$\begin{bmatrix} K_D^{*(N+1)}, & 0 & C_D^{*(N+1)} \\ 0, & K_W^{*(N+1)}, & C_W^{*(N+1)} \\ C_D^{*(N+1)^T}, & C_W^{*(N+1)^T}, & 0 \end{bmatrix} \begin{Bmatrix} \Delta q_D^* \\ \Delta q_W^* \\ T_S^* \end{Bmatrix}$$

$$= \begin{Bmatrix} \Delta \bar{T}_D^* \\ \Delta \bar{T}_W^* \\ 0 \end{Bmatrix} - \begin{Bmatrix} \epsilon_D^{*(N)} \\ \epsilon_W^{*(N)} \\ 0 \end{Bmatrix} + [A_D^*, \ -A_W^*, \ 0]\{\lambda^*\} \quad (5)$$

$$\{\lambda^*\}([A_D^*, \ -A_W^*]\{{}^{\Delta q_D^*}_{\Delta q_W^*}\} + \{h^*\}) = 0 \quad (6)$$

$$[A_D^*, \ -A_W^*]\{{}^{\Delta q_D^*}_{\Delta q_W^*}\} + \{h^*\} \geq 0 \quad (7)$$

and

$$\{\lambda^*\} \geq 0 \quad (8)$$

where ($[K_D^{*(N+1)}]$, $[K_W^{*(N+1)}]$) and ($[C_D^{*(N+1)}]$, $[C_W^{*(N+1)}]$) represent the global stiffness and friction matrix of components D and W at the $(N+1)$th load step, respectively. $\{\Delta q_D^*\}$ and $\{\Delta q_W^*\}$ are the global incremental nodal displacement vectors of components D and W from the Nth load step to the $(N+1)$th step. $\{T_S^*\}$ is the global nodal pressure vector due to friction on possible contact surfaces at the $(N+1)$th step. $\{\Delta \bar{T}_D^*\}$ and $\{\Delta \bar{T}_W^*\}$ denote the global incremental external loadings applied on components D and W from the Nth load step to the $(N+1)$th step, respectively. $\{\epsilon_D^{*(N)}\}$ and $\{\epsilon_W^{*(N)}\}$ serve to conduct an equilibrium check to reduce the cumulative errors at the Nth step. $[A_A^*, \ -A_B^*, \ 0]$ represents the gradient matrix of contact surface function $\mathfrak{F}$. $\{\lambda^*\}$ is the vector of nodal values of λ. $\{h^*\}$ represents the gap vector governing the contact behavior between components D and W.

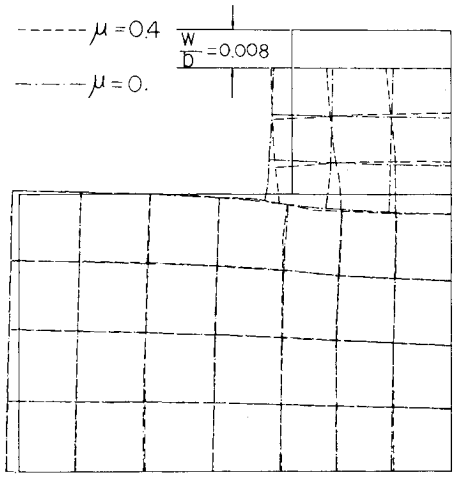

Fig. 4 Influence of friction coefficients on deformations ($R=1.0$).

Equations (5-8) can be solved by a quadratic mathematic programming technique that is well documented as, for instance, in Ref. 4.

Results and Discussion

To demonstrate the validity of the present technique, the problem of a punch with a rigid die, and without considering the effect of friction at contact surfaces, as solved in the ADINA program,[5] is considered. The geometry, loading conditions, and finite element idealization are shown in Fig. 1. The computed results for punch forces and plastic zones are in excellent agreement with ADINA's solutions, which are not shown here. To investigate the influence of material properties and friction effects, two different material properties of the deformable die and two different friction coefficients (μ) between the contact surfaces are considered. They are 1) material properties: $E_D=15{,}000$ ksi, $\sigma_{YD}=19.5$ ksi, and $\nu=0.33$; and $E_D=10{,}000$ ksi, $\sigma_{YD}=13$ ksi, and $\nu=0.33$; and 2) friction coefficients: $\mu=0$ and $\mu=0.4$. Material properties of the work piece are taken as $E_W=10{,}000$ ksi, $\sigma_{YW}=13$ ksi, and $\nu=0.33$. In the above, (E_D, E_W), (σ_{YD}, σ_{YW}), and ν represent Young's modulus, yield stresses, and Poisson's ratio of the die and work piece, respectively. The materials herein are considered as isotropic and elastic-perfectly-plastic. The geometry, loading conditions, and finite element idealization are the same as shown in Fig. 1.

Figure 2 shows the required punch forces vs various punch depths for two values of $R(R=E_D/E_W)$ and two values of friction coefficient μ. As expected for the same depth of punch, a larger punch force is needed for higher values of R, although it is not as influenced by friction effects (and friction coefficients) induced by the deformation of contact surfaces. However, the significant influence of different friction coefficients on the magnitudes of plastic zones and deformations can be seen in Figs. 3 and 4, respectively.

References

[1]Chen, W. H. and Tsai, P., "Finite Element Analysis of Elastodynamic Sliding Contact Problems with Friction," to appear

in *Computers and Structures*.

[2]Hung, N. D. and de Saxce, G., "Frictionless Contact of Elastic Bodies by Finite Element Method and Mathematical Programming Technique," *Computers and Structures*, Vol. 11, 1980, pp. 55-67.

[3]Webster, W. D. Jr. and Davis, R. L., "Development of a Friction Element for Metal Forming Analysis," *Journal of Engineering for Industry, Transactions of ASME Series B*, Vol. 104, Aug. 1982, pp. 253-256.

[4]Morris, A. J., *Foundations of Structural Optimization: A Unified Approach*, John Wiley & Sons, New York, 1982, pp. 335-358.

[5]Bathe, K. J., "ADINA—A Finite Element Program for Automatic Dynamic Incremental Nonlinear Analysis," Rept. 82448-1, Acoustic and Vibration Laboratory, Department of Mechanical Engineering, Massachusetts Insitute of Technology, Cambridge, 1975, pp. 226-228.

Transient Heat-Transfer Analysis of a Conical Cathode of an MPD Arcjet

R. C. Mehta*
Vikram Sarabhai Space Centre, Trivandrum, India

Nomenclature

A,B,C,D	= coefficients of square temperature matrix
Bi	= Biot number, hL/k
h	= heat-transfer coefficient
I	= applied current
k	= thermal conductivity
L	= cathode length
Qs	= heat transfer to cathode root
r	= cathode radius
r_o	= cathode tip radius
T	= local temperature of cathode at x
T_s	= cathode temperature at $x=0$
T_∞	= surrounding temperature
t	= nondimensional time, $\kappa\tau/L^2$
Δt	= computing time
x	= space coordinate
X	= nondimensional length, x/L
X_1	= nondimensional conical length of cathode, L_1/L
Δx	= node thickness
α	= semicone angle
ϵ	= emissivity
θ	= nondimensional temperature, T/T_s
ρ	= electrical resistivity
κ	= thermal diffusivity
σ	= Stefan-Boltzmann constant

Subscripts

i,o,R	= node identifiers
n	= designated the point $(t+\Delta t)$
$n+\frac{1}{2}$	= intermediate time level

Introduction

MOST magnetoplasmadynamic (MPD) thrusters operate at large discharge currents and low mass flow rates in order to obtain high specific impulse and thrust efficiency.[1] It is required that the cathode be operated with high temperatures at the cathode root to allow the emission of electrons with a moderate electric field while suffering minimum material loss. But severe surface erosion at the cathode tip has been observed experimentally[2,3] in transient operating conditions. In such situation, a knowledge of the temperature distribution along the cathode is essential for the thermal design of the cathode configuration. In general, 2% thoriated tungsten electrode with a semi-cone angle of 15-30 deg is employed in plasma torches and MPD arc devices.[4] A literature survey shows that transient heat-transfer analysis of the conical shape cathode has not been considered.

This Note reports a two-time level implicit scheme for the numerical solution of the nonlinear transient energy equation. As will be shown, the scheme is simple, straightforward, and unconditionally stable and convergent.

Analysis

Consider a one-dimensional cathode of conical shape with constant thermophysical properties. The configuration is as shown in Fig. 1. The nondimensional transient equation with combined conduction, ohmic heating, radiation, and convection can be written as

$$\frac{\partial^2\theta}{\partial X^2}+\frac{2\tan\alpha}{(X\tan\alpha+r_o/L)}\frac{\partial\theta}{\partial X}+\frac{I^2\rho}{kT_s[\pi(X\tan\alpha+r_o/L)]^2}-\frac{2\epsilon\sigma LT_s^3\tan\alpha}{k(X\tan\alpha+r_o/L)}\left[\theta^4-\left(\frac{T_\infty}{T_s}\right)^4\right]-\frac{2Bi\tan\alpha}{(X\tan\alpha+r_o/L)}\left[\theta-\left(\frac{T_\infty}{T_s}\right)\right]=\frac{\partial\theta}{\partial t},\quad 0<X\le X_1 \tag{1}$$

$$\frac{\partial^2\theta}{\partial X^2}+\frac{I^2\rho}{kT_s(\pi r/L)^2}-\frac{2\epsilon\sigma L^2T_s^3}{kr}\left[\theta^4-\left(\frac{T_\infty}{T_s}\right)^4\right]-\frac{2LBi}{r}\left[\theta-\left(\frac{T_\infty}{T_s}\right)\right]=\frac{\partial\theta}{\partial t},\quad X_1<X<1 \tag{2}$$

with the initial and boundary conditions

$$\theta(X,0)=T_o/T_s,\ \text{for all } X \tag{3a}$$

$$\theta(0,t)=1,\quad t>0 \tag{3b}$$

$$\frac{\partial\theta(1,t)}{\partial X}=0,\quad t>0 \tag{3c}$$

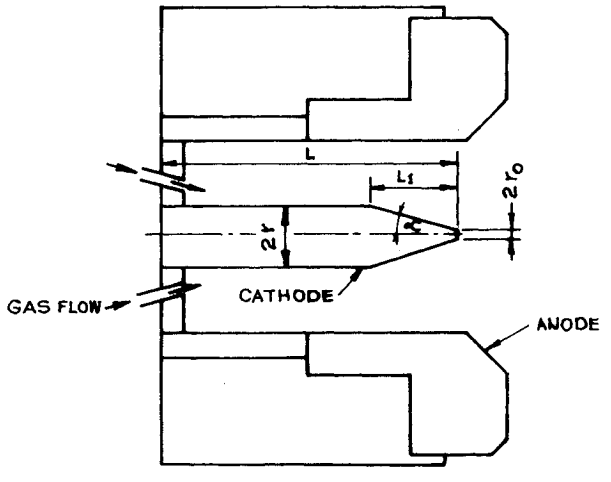

Fig. 1 Quasisteady MPD arcjet.

Received Aug. 23, 1984; revision received Jan. 14, 1985.

*Engineer, Aerodynamics Division.